NEUROSCIENCE

Intense threat switches dorsal raphe serotonin neurons to a paradoxical operational mode

Changwoo Seo[1,2]*, Akash Guru[1,2]*, Michelle Jin[1]†, Brendan Ito[1], Brianna J. Sleezer[1], Yi-Yun Ho[1,2], Elias Wang[1]‡, Christina Boada[1]§, Nicholas A. Krupa[1], Durgaprasad S. Kullakanda[1], Cynthia X. Shen[1], Melissa R. Warden[1,2]¶

Survival depends on the selection of behaviors adaptive for the current environment. For example, a mouse should run from a rapidly looming hawk but should freeze if the hawk is coasting across the sky. Although serotonin has been implicated in adaptive behavior, environmental regulation of its functional role remains poorly understood. In mice, we found that stimulation of dorsal raphe serotonin neurons suppressed movement in low- and moderate-threat environments but induced escape behavior in high-threat environments, and that movement-related dorsal raphe serotonin neural dynamics inverted in high-threat environments. Stimulation of dorsal raphe γ-aminobutyric acid (GABA) neurons promoted movement in negative but not positive environments, and movement-related GABA neural dynamics inverted between positive and negative environments. Thus, dorsal raphe circuits switch between distinct operational modes to promote environment-specific adaptive behaviors.

The decision to move or to refrain from movement depends on the structure of the environment and the internal state of the animal. Imminent threats may provoke a "fight-or-flight" response, whereas distant or uncertain threats may induce either vigilant freezing or a delayed, strategic avoidance response (*1*, *2*). Hunger may encourage travel to a distant food source, but a sated animal may not find this goal worth the energy expenditure or risk (*3*).

Neuromodulatory systems receive input from brain regions that represent environmental structure and internal state (*4*) and are essential for the coordinated regulation of the neural circuits that control movement. Whereas dopamine (DA) promotes behavioral activation in vertebrates (*5*, *6*), forebrain serotonin (5-hydroxytryptamine; 5-HT) is more strongly associated with behavioral inhibition (*7*, *8*); elevated 5-HT promotes pausing and waiting (*9*–*11*), whereas reduced 5-HT promotes impulsivity and perseverative responding (*12*, *13*). Paradoxically, selective serotonin reuptake inhibitors (SSRIs) reduce immobility in the forced swim test (FST) and tail suspension test (TST) (*14*), as does stimulation of the prefrontal-dorsal raphe nucleus (DRN) projection (*15*). We sought to investigate whether differences in environmental threat level underlie this discrepancy.

We used fiber photometry (*16*) to monitor the population dynamics of DRN 5-HT neurons in freely behaving mice (fig. S1A). We injected AAV5-CAG-FLEX-GCaMP6s (*17*) into the DRN of SERT-Cre mice (*18*) and implanted an optical fiber over the DRN (Fig. 1A and fig. S1B). Movement onset in the open field test (OFT; Fig. 1B) was associated with a robust reduction in DRN 5-HT fluorescence (Fig. 1, C to E; GFP control data, Fig. 1E and fig. S1, C to E). We then recorded DRN 5-HT activity during performance of a cued reward approach task (Fig. 1F and fig. S2, A and B), in which mice crossed an operant chamber to receive a reward, and found that activity decreased upon movement in this environment (Fig. 1, G to I; movement offset, fig. S3, A and B). We also found that DRN 5-HT activity decreased upon movement to avoid a shock in a cued avoidance task (Fig. 1, J to M, and fig. S2, C and D; movement offset, fig. S3, C and D).

Next, we examined DRN 5-HT neural activity during the TST (Fig. 2A), a high-threat environment (*19*), and observed an increase in DRN 5-HT fluorescence upon movement onset (Fig. 2, B to D; GFP data, Fig. 2D and fig. S1, F to H; movement offset, fig. S3, E and F). We also observed an increase in DRN 5-HT fluorescence upon movement onset in escape (failed) trials in the avoidance task (Fig. 2, E and F), during which mice were also in direct contact with the stressor. Finally, we microendoscopically recorded DRN 5-HT activity (*20*) and observed similar environment-dependent switching of movement dynamics in single DRN 5-HT neurons (figs. S4 and S5). Thus, DRN 5-HT neural activity decreases upon movement initiation in low- or moderate-threat environments, but high-threat, escape-provoking environments invert this response.

To probe the causal role of DRN 5-HT neurons in regulating movement in different environments, we optogenetically (*21*) activated 5-HT neurons (Fig. 3A and fig. S6A) during these behaviors. Optical stimulation of DRN 5-HT neurons reduced speed in the OFT [Fig. 3, B and C; ChR2, 3.67 ± 0.31 cm/s; enhanced yellow fluorescent protein (eYFP), 5.16 ± 0.44 cm/s], as expected (*10*). Speed decreased upon stimulation in both approach and avoidance tasks (approach: Fig. 3, D and E, and fig. S6, B and C; ChR2, 3.0 ± 0.3 cm/s; eYFP, 7.1 ± 1.0 cm/s; avoidance: Fig. 3, G and H, and fig. S6, D and E; ChR2, 2.2 ± 0.4 cm/s; eYFP, 3.8 ± 0.4 cm/s), and latency to chamber crossing was greater in stimulated animals in both tasks (Fig. 3, F and I). TST stimulation in the same mice produced an increase in movement (Fig. 3, J to L). These data provide causal evidence for a switch in DRN 5-HT neuron function from suppression to facilitation of movement in high-threat escape conditions.

We then investigated the movement-related dynamics of DRN GABA neurons using fiber photometry in Vgat-ires-Cre mice (*22*) (fig. S7, A and B, and fig. S8). Activity decreased upon movement to cross the chamber in the approach task (Fig. 4, A to C; movement offset, fig. S3, G and H) but increased upon movement to cross the chamber in the avoidance task (Fig. 4, F to H; movement offset, fig. S3, I and J), switching at a lower threat level than DRN 5-HT neurons. Recordings during avoidance training revealed rapid switching after the first few shocks (figs. S9 and S10).

Approach and avoidance differ in environmental valence, and we found that movement-related dynamics also switched in other valenced environments. Wheel running (Fig. 4K) induced a reduction in DRN GABA activity (Fig. 4, L to N; GFP data, Fig. 4N and fig. S7, C to E), but DRN GABA neural activity increased upon movement during the TST (Fig. 4, P to S; GFP data, Fig. 4S and fig. S7, F to H; movement offset, fig. S3, K and L) and upon movement in escape (failed) trials in the avoidance task (fig. S7, I to L).

Finally, we investigated whether DRN GABA neurons have a causal role in movement regulation. Optogenetic stimulation of GABA DRN neurons (fig. S11, A and B) had no impact on speed (Fig. 4, D and E, and fig. S11, C and D; ChR2, 7.3 ± 0.7 m/s; eYFP, 6.7 ± 1.0 m/s), nor on latency to chamber crossing (fig. S11E) in the approach task or on wheel mobility (Fig. 4O), but stimulation in these same mice induced higher speed in the OFT (fig. S12, A to D). Stimulation increased speed (Fig. 4, I and J, and fig. S11, F and G; ChR2, 7.7 ± 0.7 m/s; eYFP, 4.0 ± 0.2 m/s) and reduced latency (fig. S11H) in the avoidance task, and increased movement in the TST (Fig. 4T), thereby revealing a causal role for DRN GABA neurons in promoting movement in environments with negative valence.

These findings show that changes in environmental threat intensity and valence switch the functional roles of DRN 5-HT and GABA neurons

[1]Department of Neurobiology and Behavior, Cornell University, Ithaca, NY 14853, USA. [2]Cornell Neurotech, Cornell University, Ithaca, NY 14853, USA.
*These authors contributed equally to this work. †Present address: Neurobiology of Relapse Section, National Institute on Drug Abuse (NIDA) Intramural Research Program, Baltimore, MD 21224, USA. ‡Present address: Department of Electrical Engineering, Stanford University, Stanford, CA 94305, USA. §Present address: School of Medicine, New York University, New York, NY 10016, USA.
¶Corresponding author. Email: mrwarden@cornell.edu

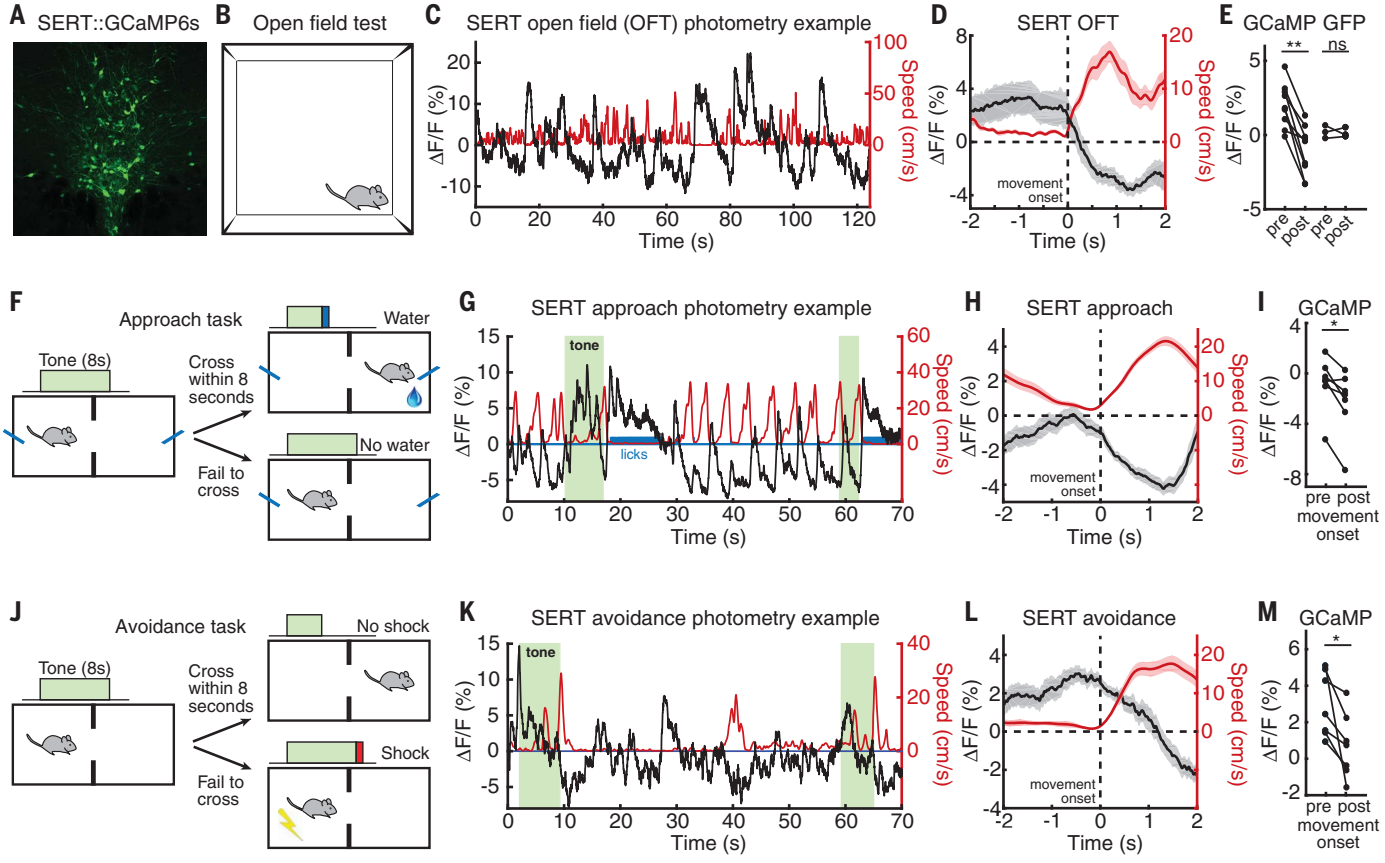

Fig. 1. DRN 5-HT neural activity decreases upon movement in low- or moderate-threat environments. (**A**) GCaMP6s expression in DRN 5-HT neurons in a SERT-Cre mouse. (**B**) OFT schematic. (**C**) Example OFT photometry from a SERT::GCaMP6s mouse. Black, GCaMP Δ*F/F*; red, speed. (**D**) Mean Δ*F/F* aligned to OFT movement onset. (**E**) Mean Δ*F/F* before and after OFT movement onset in GCaMP (n = 9) and GFP (n = 3) mice. (**F**) Approach task schematic. (**G**) Example approach photometry from the same mouse. (**H**) Mean Δ*F/F* aligned to approach movement onset. (**I**) Mean Δ*F/F* before and after approach movement onset in GCaMP (n = 7) mice. (**J**) Avoidance task schematic. (**K**) Example avoidance photometry data from the same mouse. (**L**) Mean Δ*F/F* aligned to avoidance movement onset. (**M**) Mean Δ*F/F* before and after avoidance movement onset in GCaMP (n = 7) mice. *P < 0.05, **P < 0.01 (Wilcoxon signed-rank test); ns, not significant. Shaded areas in (D), (H), and (L) indicate SEM.

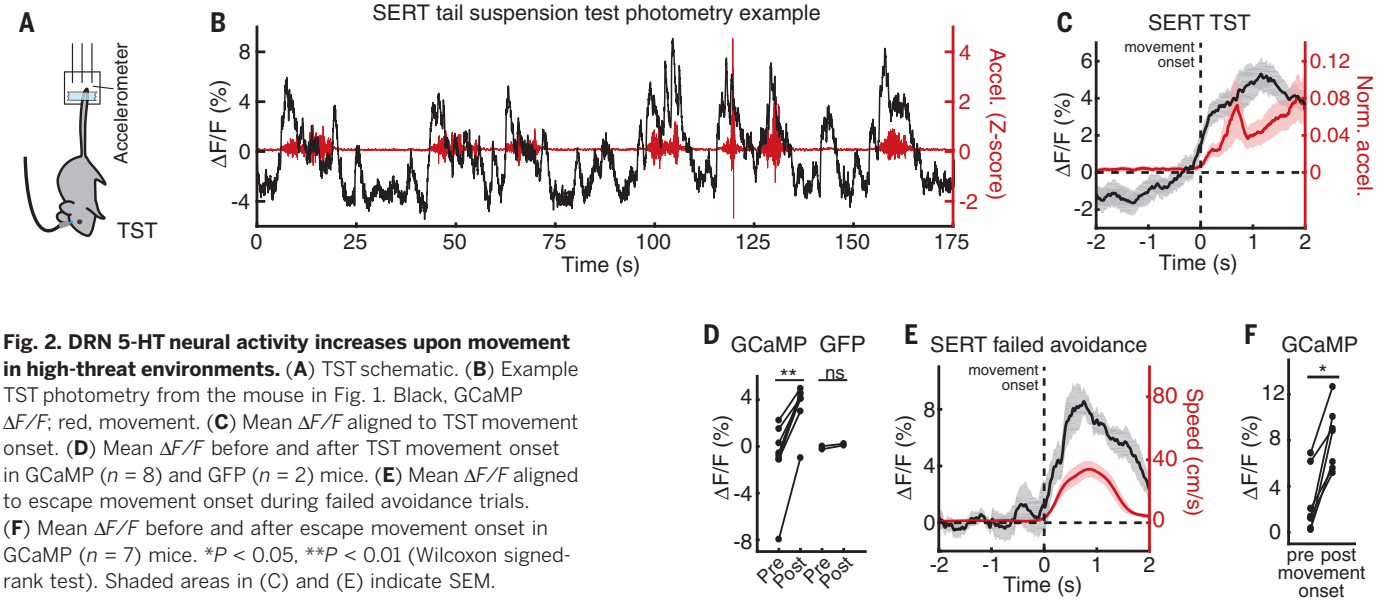

Fig. 2. DRN 5-HT neural activity increases upon movement in high-threat environments. (**A**) TST schematic. (**B**) Example TST photometry from the mouse in Fig. 1. Black, GCaMP Δ*F/F*; red, movement. (**C**) Mean Δ*F/F* aligned to TST movement onset. (**D**) Mean Δ*F/F* before and after TST movement onset in GCaMP (n = 8) and GFP (n = 2) mice. (**E**) Mean Δ*F/F* aligned to escape movement onset during failed avoidance trials. (**F**) Mean Δ*F/F* before and after escape movement onset in GCaMP (n = 7) mice. *P < 0.05, **P < 0.01 (Wilcoxon signed-rank test). Shaded areas in (C) and (E) indicate SEM.

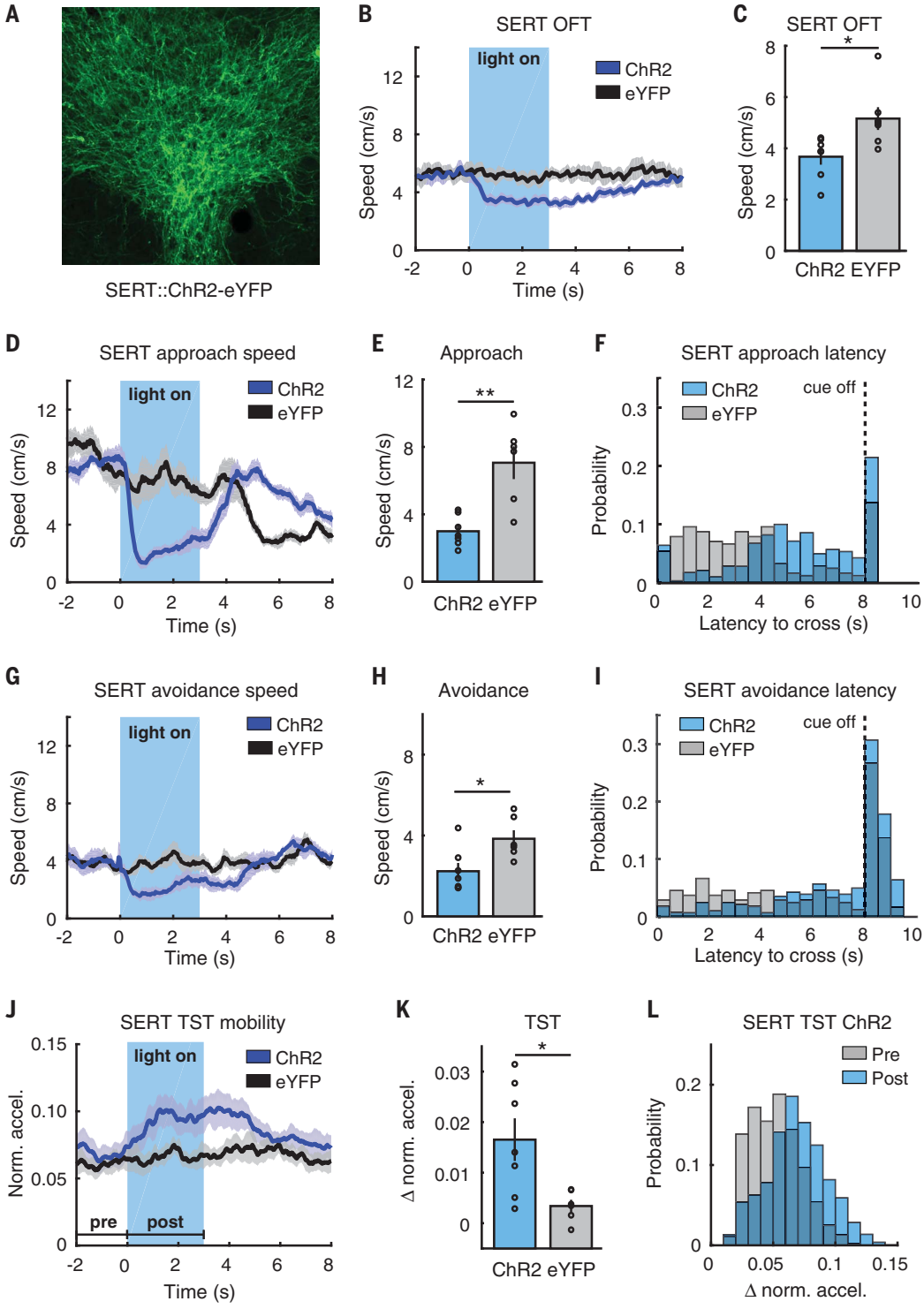

Fig. 3. DRN 5-HT stimulation suppresses or promotes movement at different threat levels. (**A**) ChR2-eYFP expression in DRN 5-HT neurons in a SERT-Cre mouse. (**B**) Speed aligned to light onset, OFT (SERT::ChR2-eYFP, $n = 7$; SERT::eYFP, $n = 7$). (**C**) Mean speed during stimulation, OFT. (**D**) Speed aligned to light/cue onset, approach task (SERT::ChR2-eYFP, $n = 7$; SERT::eYFP, $n = 6$). (**E**) Mean speed during stimulation, approach task. (**F**) Latency to cross, approach task. $P < 0.0001$ (log-rank test). (**G**) Speed aligned to light/cue onset, avoidance task (SERT::ChR2-eYFP, $n = 7$; SERT::eYFP, $n = 6$). (**H**) Mean speed during stimulation, avoidance task. (**I**) Latency to cross distribution, avoidance task. $P < 0.0001$ (log-rank test). (**J**) Movement aligned to light onset, TST (SERT::ChR2-eYFP, $n = 7$; SERT::eYFP, $n = 6$). (**K**) Mean difference between pre- and post-light onset movement, TST. (**L**) SERT::ChR2-eYFP movement before and after light onset, TST. $^{*}P < 0.05$, $^{**}P < 0.01$ (Wilcoxon rank sum test). Shaded areas in (B), (D), (G), and (J) and vertical lines in (C), (E), (H), and (K) indicate SEM.

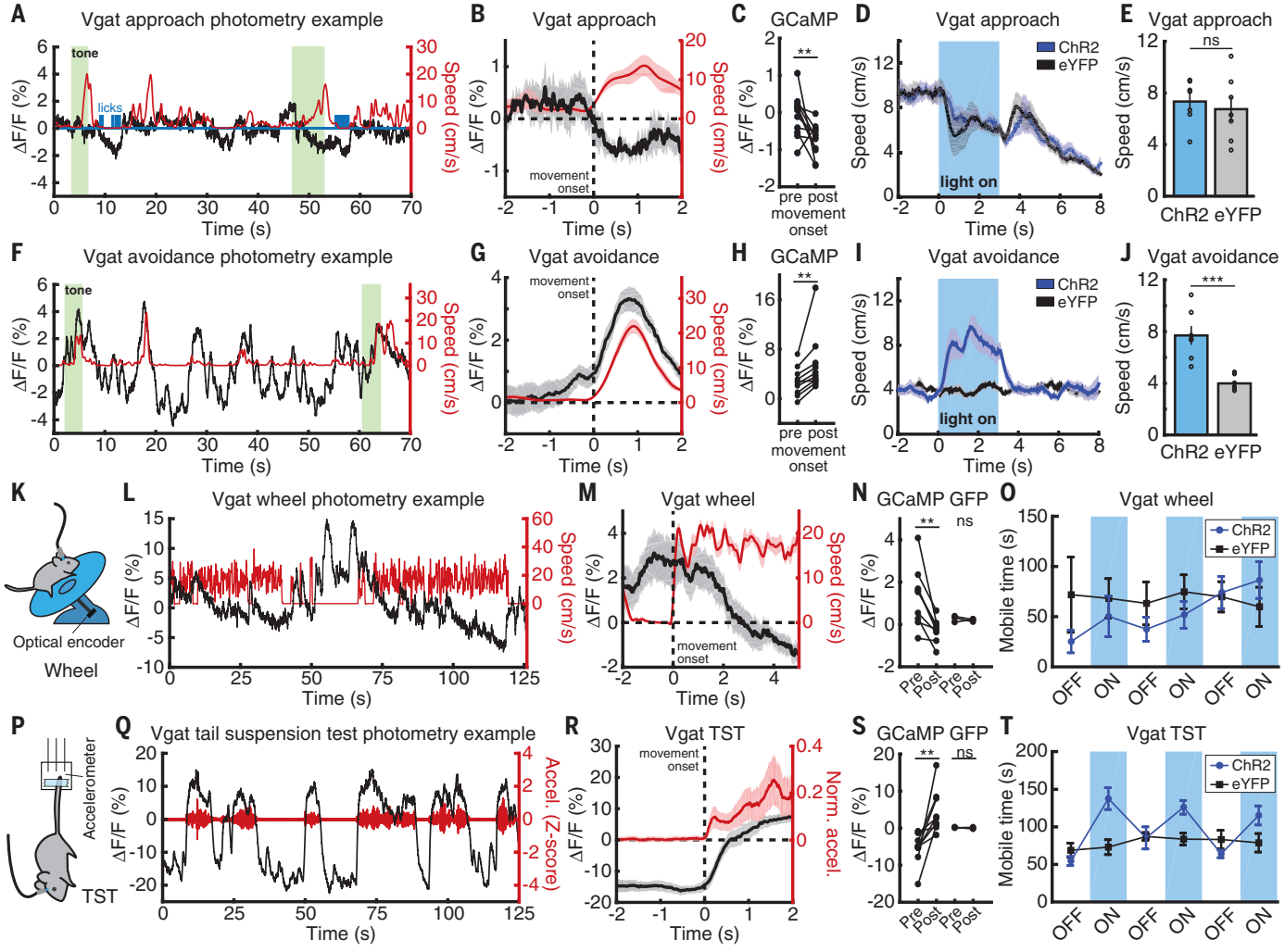

Fig. 4. DRN GABA stimulation promotes movement in environments with negative valence. (**A**) Approach photometry example from a Vgat::GCaMP6s mouse. Black, GCaMP Δ*F*/*F*; red, speed. (**B**) Mean Δ*F*/*F* aligned to approach movement onset. (**C**) Mean Δ*F*/*F* before and after approach movement onset (n = 11). (**D**) Speed aligned to stimulation/cue onset, approach (Vgat::ChR2-eYFP, n = 8; Vgat::eYFP, n = 7). (**E**) Mean speed during stimulation, approach. (**F**) Example avoidance photometry. (**G**) Mean Δ*F*/*F* aligned to avoidance movement onset. (**H**) Mean Δ*F*/*F* before and after avoidance movement onset (n = 10). (**I**) Speed aligned to stimulation/cue onset, avoidance (Vgat::ChR2-eYFP, n = 8; Vgat::eYFP, n = 7). (**J**) Mean speed during stimulation, avoidance. (**K**) Wheel schematic. (**L**) Example wheel photometry. (**M**) Mean Δ*F*/*F* aligned to wheel movement onset. (**N**) Mean Δ*F*/*F* before and after wheel movement onset in GCaMP (n = 9) and GFP (n = 3) mice. (**O**) Mean mobile time in 3-min stimulation or nonstimulation blocks, wheel (Vgat::ChR2-eYFP, n = 7; Vgat::eYFP, n = 7; P = 0.9015, Wilcoxon rank sum test). (**P**) TST schematic. (**Q**) TST photometry example. (**R**) Mean Δ*F*/*F* aligned to TST movement onset. (**S**) Mean Δ*F*/*F* before and after TST movement onset in GCaMP (n = 9) and GFP (n = 3) mice. (**T**) Mean mobile time in 3-min stimulation or nonstimulation blocks, TST (Vgat::ChR2-eYFP, n = 7; Vgat::eYFP, n = 7; P = 0.007, Wilcoxon rank sum test). $^{**}P < 0.01$, $^{***}P < 0.001$ [Wilcoxon signed-rank test (photometry) or Wilcoxon rank sum test (optogenetics)]. Shaded areas in (B), (G), (M), and (R) and vertical lines in (E), (J), (O), and (T) indicate SEM.

in movement regulation. The notion that movement in states of extreme threat may be differently regulated is not without precedent. Paradoxical kinesia has been observed in akinetic Parkinsonian patients (*23*), and DA-depleted akinetic rats attempt escape in deep water (*24*), suggesting alternative motor regulation in fight-or-flight situations. DRN function during stress is regulated by a number of systems that may play a role in environment-dependent functional switching; SSRI-induced TST immobility reduction requires DRN norepinephrine (*25*); DRN corticotropin-releasing factor inhibits 5-HT release and promotes active coping or the reverse, depending on stress history (*26*, *27*); and DRN activation is dampened by prefrontal activity during controllable stress (*28*).

Our experiments probed the neural dynamics and functional roles of two distinct DRN cell types in movement regulation. Our findings show that urgent escape conditions switch DRN 5-HT neurons from suppression of movement to facilitation, and that DRN GABA neurons selectively facilitate movement in environments with negative valence, consistent with the neural dynamics that we observed in both cell types. These results reveal a role for DRN circuits in rapid, environment-specific behavioral regulation.

REFERENCES AND NOTES

1. M. S. Fanselow, *Psychon. Bull. Rev.* **1**, 429–438 (1994).
2. G. De Franceschi, T. Vivattanasarn, A. B. Saleem, S. G. Solomon, *Curr. Biol.* **26**, 2150–2154 (2016).
3. R. C. Ydenberg, L. M. Dill, *Adv. Stud. Behav.* **16**, 229–249 (1986).
4. S. K. Ogawa, J. Y. Cohen, D. Hwang, N. Uchida, M. Watabe-Uchida, *Cell Rep.* **8**, 1105–1118 (2014).
5. Y. Niv, N. D. Daw, D. Joel, P. Dayan, *Psychopharmacology* **191**, 507–520 (2007).
6. J. D. Salamone *et al.*, *Curr. Top. Behav. Neurosci.* **27**, 231–257 (2016).
7. P. Soubrié, *Behav. Brain Sci.* **9**, 319 (1986).
8. J. F. W. Deakin, F. G. Graeff, *J. Psychopharmacol.* **5**, 305–315 (1991).
9. K. W. Miyazaki *et al.*, *Curr. Biol.* **24**, 2033–2040 (2014).
10. P. A. Correia *et al.*, *eLife* **6**, e20975 (2017).

11. C. A. Marcinkiewcz *et al*., *Nature* **537**, 97–101 (2016).
12. A. A. Harrison, B. J. Everitt, T. W. Robbins, *Psychopharmacology* **133**, 329–342 (1997).
13. H. F. Clarke, J. W. Dalley, H. S. Crofts, T. W. Robbins, A. C. Roberts, *Science* **304**, 878–880 (2004).
14. J. F. Cryan, A. Markou, I. Lucki, *Trends Pharmacol. Sci.* **23**, 238–245 (2002).
15. M. R. Warden *et al*., *Nature* **492**, 428–432 (2012).
16. L. A. Gunaydin *et al*., *Cell* **157**, 1535–1551 (2014).
17. T.-W. Chen *et al*., *Nature* **499**, 295–300 (2013).
18. X. Zhuang, J. Masson, J. A. Gingrich, S. Rayport, R. Hen, *J. Neurosci. Methods* **143**, 27–32 (2005).
19. K. G. Commons, A. B. Cholanians, J. A. Babb, D. G. Ehlinger, *ACS Chem. Neurosci.* **8**, 955–960 (2017).
20. Y. Ziv *et al*., *Nat. Neurosci.* **16**, 264–266 (2013).
21. E. S. Boyden, F. Zhang, E. Bamberg, G. Nagel, K. Deisseroth, *Nat. Neurosci.* **8**, 1263–1268 (2005).
22. L. Vong *et al*., *Neuron* **71**, 142–154 (2011).
23. L. Bonanni, A. Thomas, M. Onofrj, *Mov. Disord.* **25**, 1302–1304 (2010).
24. J. F. Marshall, D. Levitan, E. M. Stricker, *J. Comp. Physiol. Psychol.* **90**, 536–546 (1976).
25. O. F. O'Leary, A. J. Bechtholt, J. J. Crowley, R. J. Valentino, I. Lucki, *Eur. Neuropsychopharmacol.* **17**, 215–226 (2007).
26. M. Waselus, C. Nazzaro, R. J. Valentino, E. J. Van Bockstaele, *Biol. Psychiatry* **66**, 76–83 (2009).
27. S. Puglisi-Allegra, D. Andolina, *Behav. Brain Res.* **277**, 58–67 (2015).
28. J. Amat *et al*., *Nat. Neurosci.* **8**, 365–371 (2005).

ACKNOWLEDGMENTS

We thank T. J. Davidson and C. B. Schaffer for photometry advice; P. Dayan, I. T. Ellwood, R. M. Harris-Warrick, R. R. Hoy, J. H. Goldberg, J. R. Fetcho, E. Troconis, and D. A. Bulkin for helpful discussions and/or comments on the manuscript; T. Bollu for technical advice; G. Paquelet for microendoscopy advice; U. Lee for contributions to figure design; A. K. Recknagel for expert technical assistance; and the Warden laboratory and Cornell Neurobiology and Behavior for training and support. **Funding:** Supported by the Mong Family Foundation (C.S., Y.-Y.H., A.G.), the Taiwan Ministry of Education (Y.-Y.H.), NIH DP2MH109982 (M.R.W.), the Alfred P. Sloan Foundation (M.R.W.), the Whitehall Foundation (M.R.W.), and the Brain and Behavior Research Foundation (M.R.W.). M.R.W. is a Robertson Neuroscience Investigator–New York Stem Cell Foundation. **Author contributions:** C.S. and M.R.W. conceived the project and designed the experiments; C.S., M.J., B.I., B.J.S., C.B., and N.A.K. performed stereotaxic surgery and histology; C.S., M.J., C.B., N.A.K., and D.S.K. conducted photometry and optogenetic experiments; A.G., B.I., B.J.S., and C.S. conducted single cell physiology experiments; C.S. and Y.-Y.H. developed the behavioral data acquisition methods; C.S., A.G., B.J.S., M.J., E.W., C.X.S., and M.R.W. analyzed the data; C.S. and M.R.W. prepared the manuscript; and M.R.W. supervised all aspects of the work. **Competing interests:** The authors declare no competing financial interests. **Data and materials availability:** All data are available in the manuscript or the supplementary materials. We thank the University of North Carolina vector core for the ChR2, eYFP, and GFP vectors; the University of Pennsylvania vector core for the GCaMP6s vector; and the Stanford vector core for the GCaMP6m vector. These were made available under a material transfer agreement.

SUPPLEMENTARY MATERIALS

www.sciencemag.org/content/363/6426/538/suppl/DC1
Materials and Methods
Figs. S1 to S12
Table S1
References (*29*, *30*)

9 August 2018; accepted 4 January 2019
10.1126/science.aau8722

Intense threat switches dorsal raphe serotonin neurons to a paradoxical operational mode

Changwoo Seo, Akash Guru, Michelle Jin, Brendan Ito, Brianna J. Sleezer, Yi-Yun Ho, Elias Wang, Christina Boada, Nicholas A. Krupa, Durgaprasad S. Kullakanda, Cynthia X. Shen and Melissa R. Warden

Science **363** (6426), 538-542.
DOI: 10.1126/science.aau8722

Flipping behavior under threat

Could it be that the brain in a state of emergency or under intense threat operates in a fundamentally different way? Seo *et al.* found that mice paused when serotonin neurons were transiently stimulated in low- or medium-threat environments, but when this same neural population was stimulated in high-threat environments, mice tried to escape. Recordings from these neurons indicated that movement-related neural tuning flipped between environments. Neural activity decreased when movement was initiated in low-threat environments but increased in high-threat environments.

Science, this issue p. 538